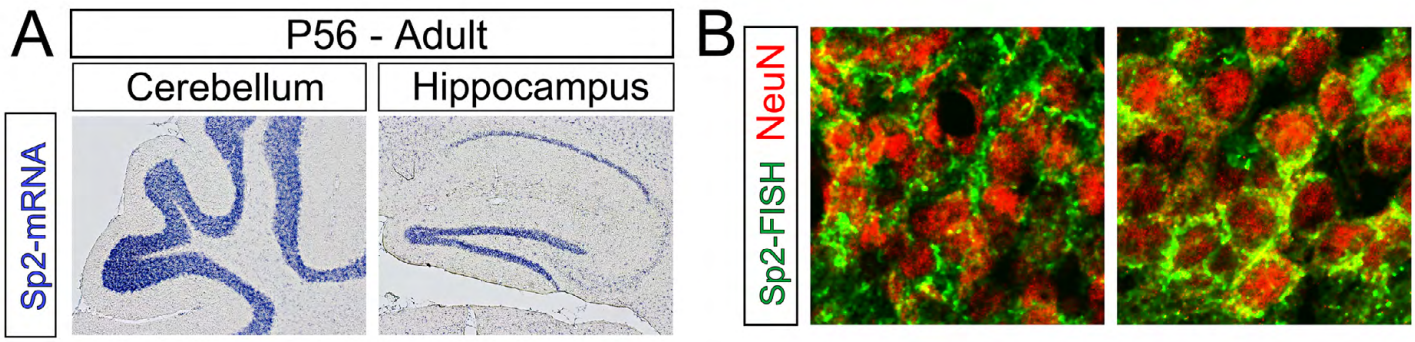

Fig. S1. Sp2 expression in the cerebellum and hippocampus of a P56 adult mouse. (**A**) *Sp2* is expressed in granular layers of the cerebellum and hippocampus in sagittal sections processed to visualize a DIG-labeled *Sp2* probe (blue). (**B**) Fluorescence in situ hybridization against the *Sp2* probe (green) co-labeled with NeuN (red) in corresponding granular layer of the cerebellum and the dentate gyrus of the hippocampus.

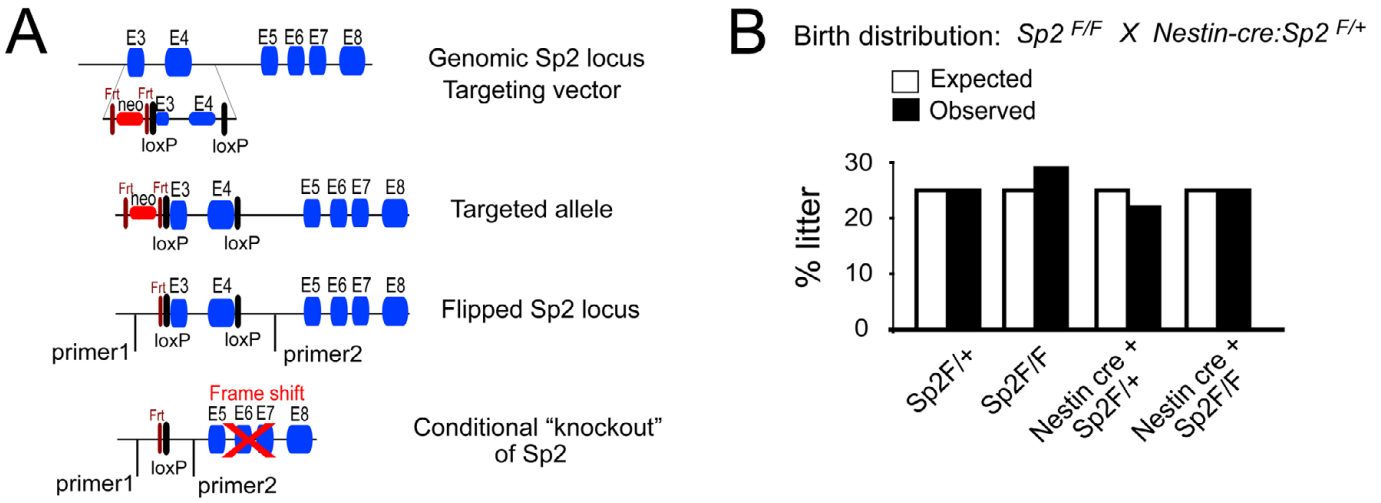

Fig. S2. Generation and analysis of the *Sp2* floxed mice. (**A**) A targeting vector containing an HSVtk-neo cassette (red bar) upstream of *Sp2* exon 3 was generated. LoxP sites (black boxes) were introduced to flank *Sp2* exon 3 and exon 4. Frt sites on both sides of the neo cassette allowed for its removal in targeted ES cells using flip-mediated recombination. Mice carrying the *Sp2* 'floxed' locus were interbred with *Nestin-cre* transgenic mice, which resulted in deletion of exons 3 and 4 in tissue harvested from the postnatal brain. (**B**) Birth rate of offspring from [*Sp2* $^{F/F}$] crossed to [*Nestin-cre(het):Sp2*$^{F/+}$] mice. The expected genotypes based on Mendelian ratios are 25% for genotypes [Sp2$^{F/+}$], [Sp2 $^{F/F}$], [*Nestin-cre(het):Sp2*$^{F/+}$] and [*Nestin-cre(het):Sp2*$^{F/F}$]. Percentages were calculated for the total number of mice (*n*=203, from 22 litters).

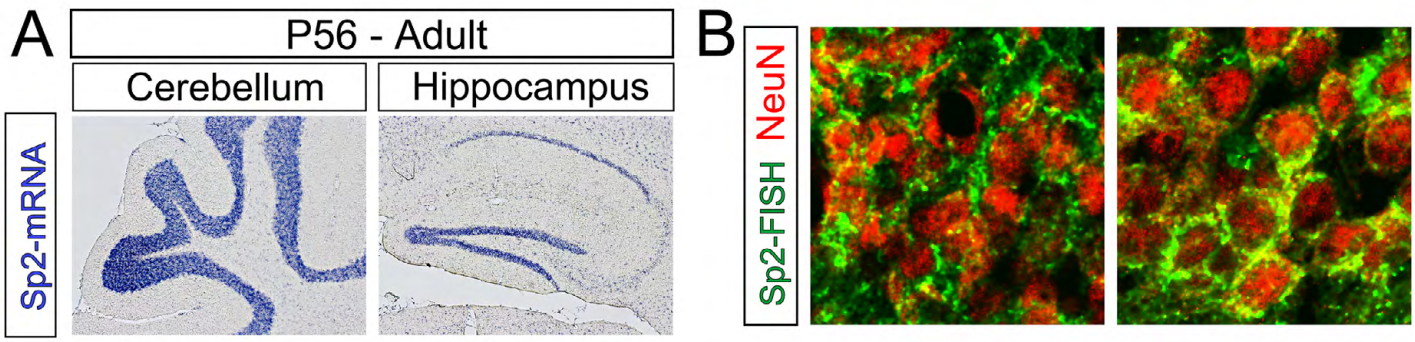

Fig. S1. Sp2 expression in the cerebellum and hippocampus of a P56 adult mouse. (**A**) *Sp2* is expressed in granular layers of the cerebellum and hippocampus in sagittal sections processed to visualize a DIG-labeled *Sp2* probe (blue). (**B**) Fluorescence in situ hybridization against the *Sp2* probe (green) co-labeled with NeuN (red) in corresponding granular layer of the cerebellum and the dentate gyrus of the hippocampus.

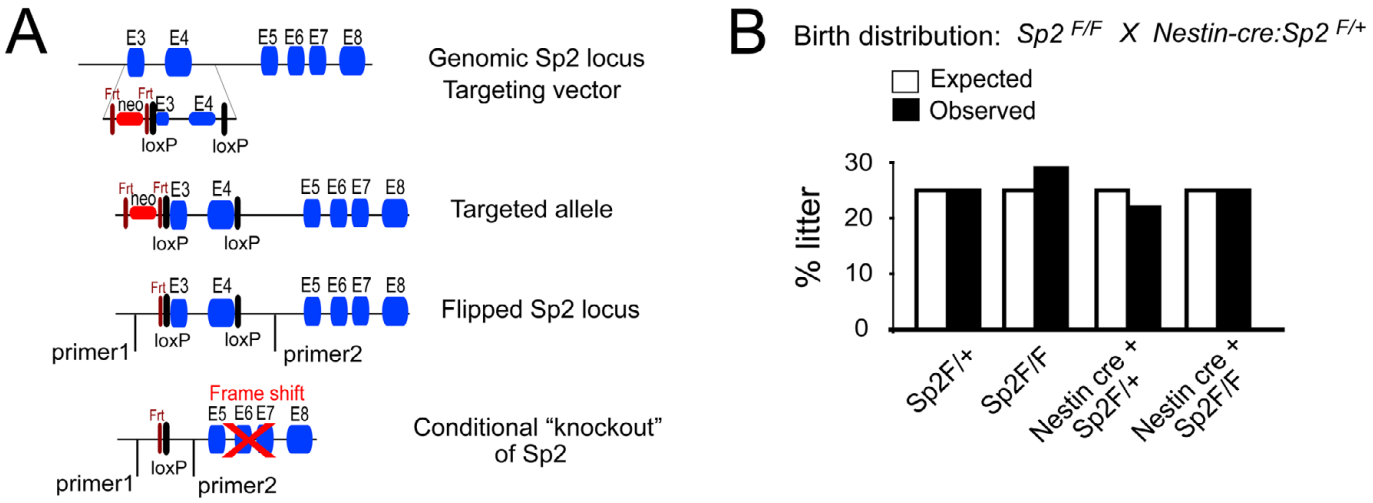

Fig. S2. Generation and analysis of the *Sp2* floxed mice. (**A**) A targeting vector containing an HSVtk-neo cassette (red bar) upstream of *Sp2* exon 3 was generated. LoxP sites (black boxes) were introduced to flank *Sp2* exon 3 and exon 4. Frt sites on both sides of the neo cassette allowed for its removal in targeted ES cells using flip-mediated recombination. Mice carrying the *Sp2* 'floxed' locus were interbred with *Nestin-cre* transgenic mice, which resulted in deletion of exons 3 and 4 in tissue harvested from the postnatal brain. (**B**) Birth rate of offspring from [*Sp2* $^{F/F}$] crossed to [*Nestin-cre(het):Sp2*$^{F/+}$] mice. The expected genotypes based on Mendelian ratios are 25% for genotypes [Sp2$^{F/+}$], [Sp2 $^{F/F}$], [*Nestin-cre(het):Sp2*$^{F/+}$] and [*Nestin-cre(het):Sp2*$^{F/F}$]. Percentages were calculated for the total number of mice (*n*=203, from 22 litters).

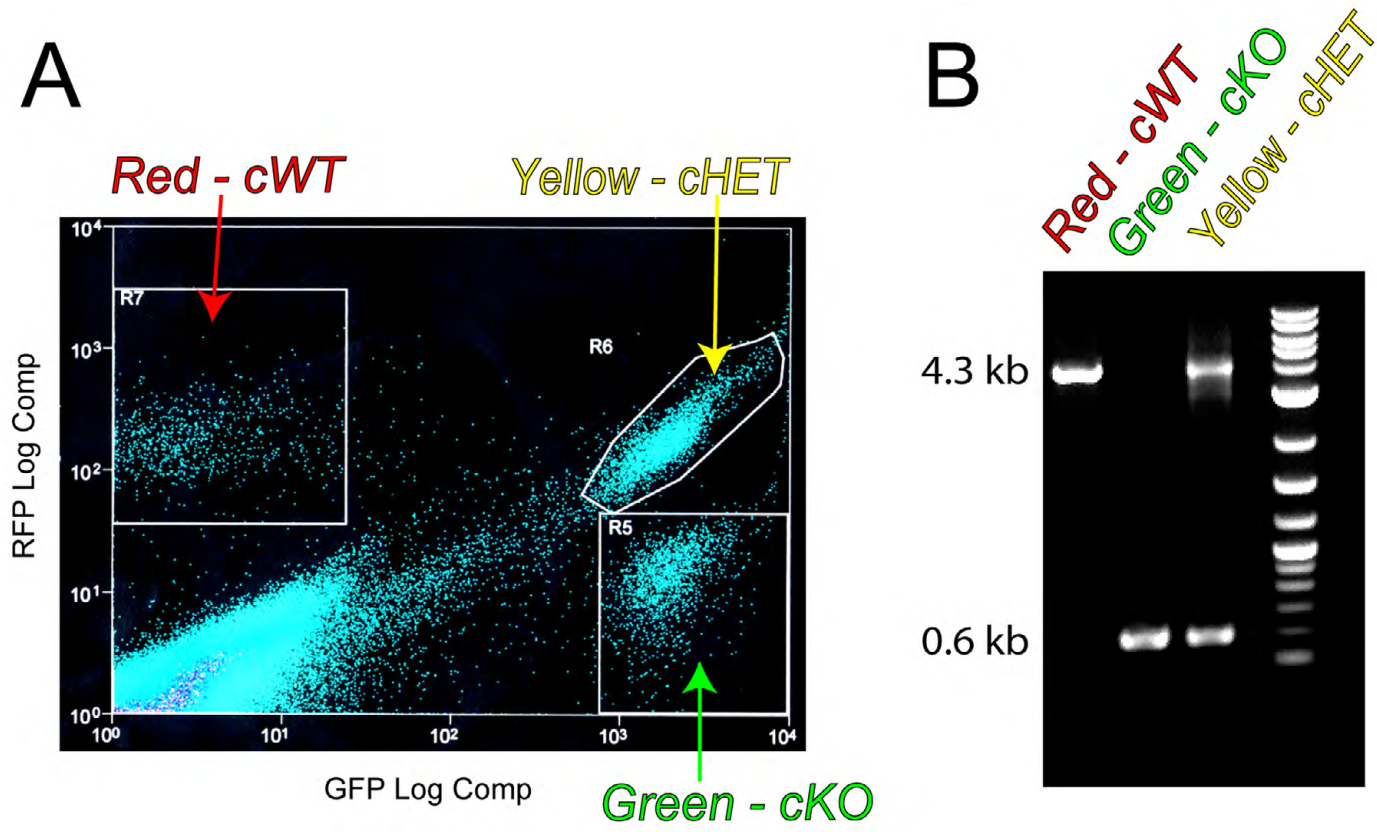

Fig. S3. Distinctly labeled MADM-11 cells faithfully carry allelic deletion of *Sp2* corresponding to expected combinatorial expression of fluorophores. (**A**) *Nestin-cre:Sp2* $^{F/+}$*:MADM-11* cells from P0 mice were harvested and isolated using fluorescence activated cell sorting. (**B**) PCR analysis of DNA confirmed genotypes of distinctly sorted populations corresponding to red=cWT, green=cKO and yellow=cHet genotypes.

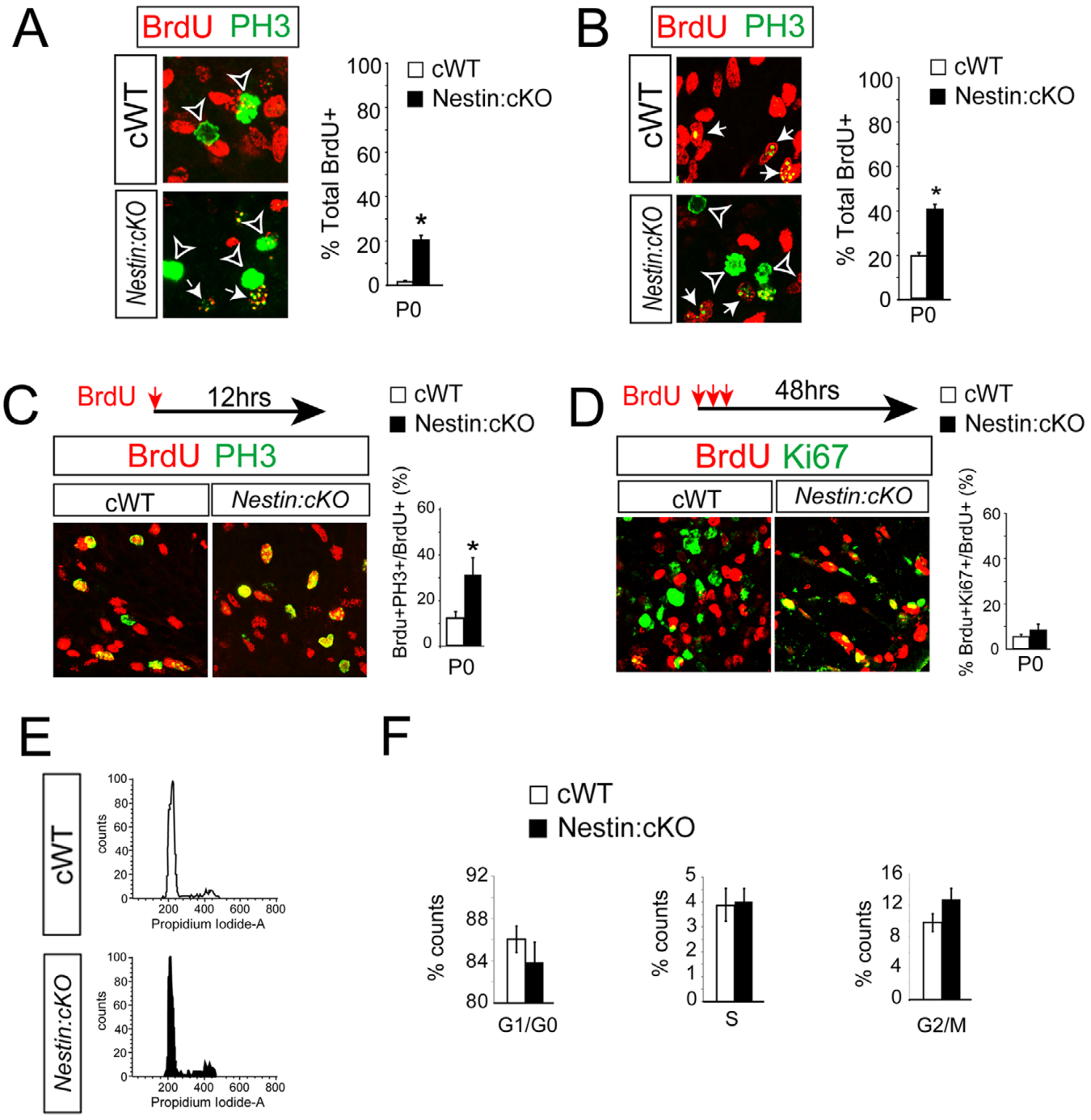

Fig. S4. Cell cycle progression from S-to-G2/M is disrupted in Nestin:cKO progenitors harvested at P0. (**A**) A 1-hour BrdU pulse-chase experiments allowed for identification of proliferating cells that progressed from S to G2/M phases of the cell cycle by co-labeling BrdU (red) with the M-phase marker PH3 (green; arrows). M-phase cells that did not incorporate BrdU during the 1-hour chase period were labeled as PH3+/BrdU negative (arrow heads). The proportion of BrdU+ cells in the SEZ and RMS of Nestin:cKO mice that progressed into G2/M (PH3+) was consistently and significantly higher compared with cWT progenitors at P0. (**B**) Four-hour BrdU pulse-chase experiments allowed for identification of proliferating Nestin:cKO progenitors that exhibit M phase perdurance. Arrows indicate BrdU+/PH3+ cells; arrowheads indicate BrdU-negative/PH3+ cells. Percentage of BrdU+/PH3+ cells among all BrdU incorporated cells is significantly increased in P0 mutant compared with the control. In addition, a significant fraction of PH3+ cells in the Nestin:cKO SEZ and RMS remained BrdU negative. (**C**) BrdU administration followed by 12 hours of chase allowed for indexing M-phase exiting. The percentage of BrdU+/PH3+ cells in the Nestin:cKO SEZ and RMS was significantly higher than in cWT brains. (**D**) To quantify cell cycle exiting, three pulses of BrdU were administered every 2 hours followed by a 48-hour survival period. In this regimen, BrdU immunoreactivity was combined with Ki67 staining in order to distinguish progenitors that had remained in, or re-entered, the cell cycle after 48 hours (BrdU+/Ki67+) from cells that had exited the cell cycle (BrdU+/Ki67 negative). Percentage of BrdU+/Ki67+ cells among all BrdU incorporated cells is higher in the Nestin:cKO SEZ/RMS compared with controls. For A-D, data are mean±s.e.m.; *P<0.05, Student's t-test, n=3/age group. (**E**,**F**) Flow cytometry for cell cycle analysis at P0. Data from cycling cells harvested from P0 SEZ and RMS illustrated higher proportion of cells in the G2/M phases in Nestin:cKOs. *P<0.01, Student's t-test, n=3/age group.

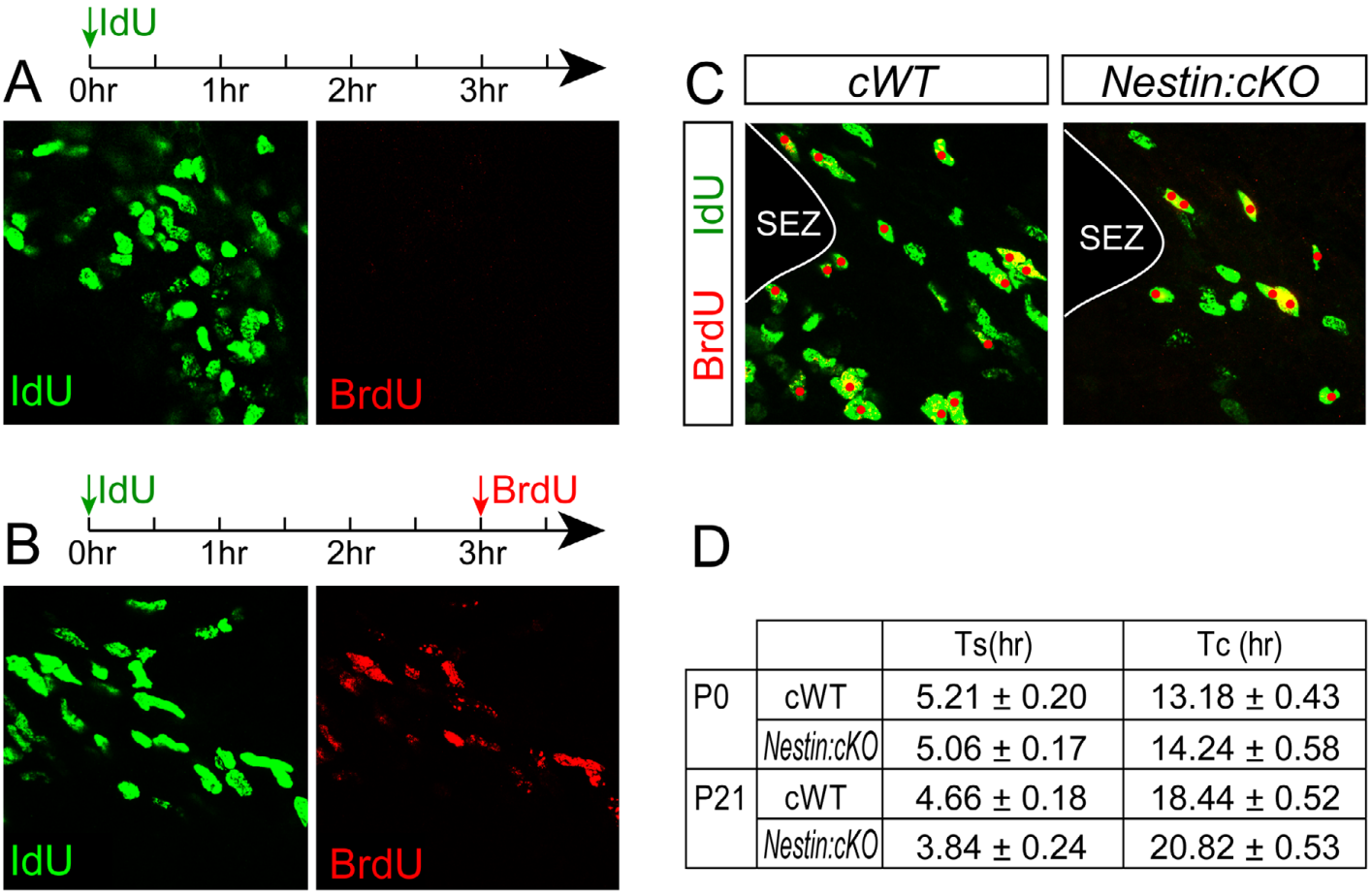

		Ts(hr)	Tc (hr)
P0	cWT	5.21 ± 0.20	13.18 ± 0.43
	Nestin:cKO	5.06 ± 0.17	14.24 ± 0.58
P21	cWT	4.66 ± 0.18	18.44 ± 0.52
	Nestin:cKO	3.84 ± 0.24	20.82 ± 0.53

Fig. S5. IdU/BrdU dual labeling for estimating the lengths of the S-phase and total cell cycle. (**A**) An antibody specific to BrdU failed to label IdU incorporated cells (green) in the absence of BrdU injection. (**B**) A pulse of IdU was followed by a pulse of BrdU 3 hours later that could be distinguished using an antibody that recognizes both BrdU and IdU (green), and one that is specific to BrdU (red). (**C**) Representative confocal micrographs of IdU (green) and BrdU (red) labeled nuclei in P21 cWT and Nestin:cKO SEZs. Red dots highlight IdU+/BrdU+ cells. (**D**) Estimated lengths of S (Ts) and total cell cycle (Tc) in the P0 and P21 wild-type and mutant SEZ progenitors. Data are mean±s.e.m., *n*=3/genotype/age.

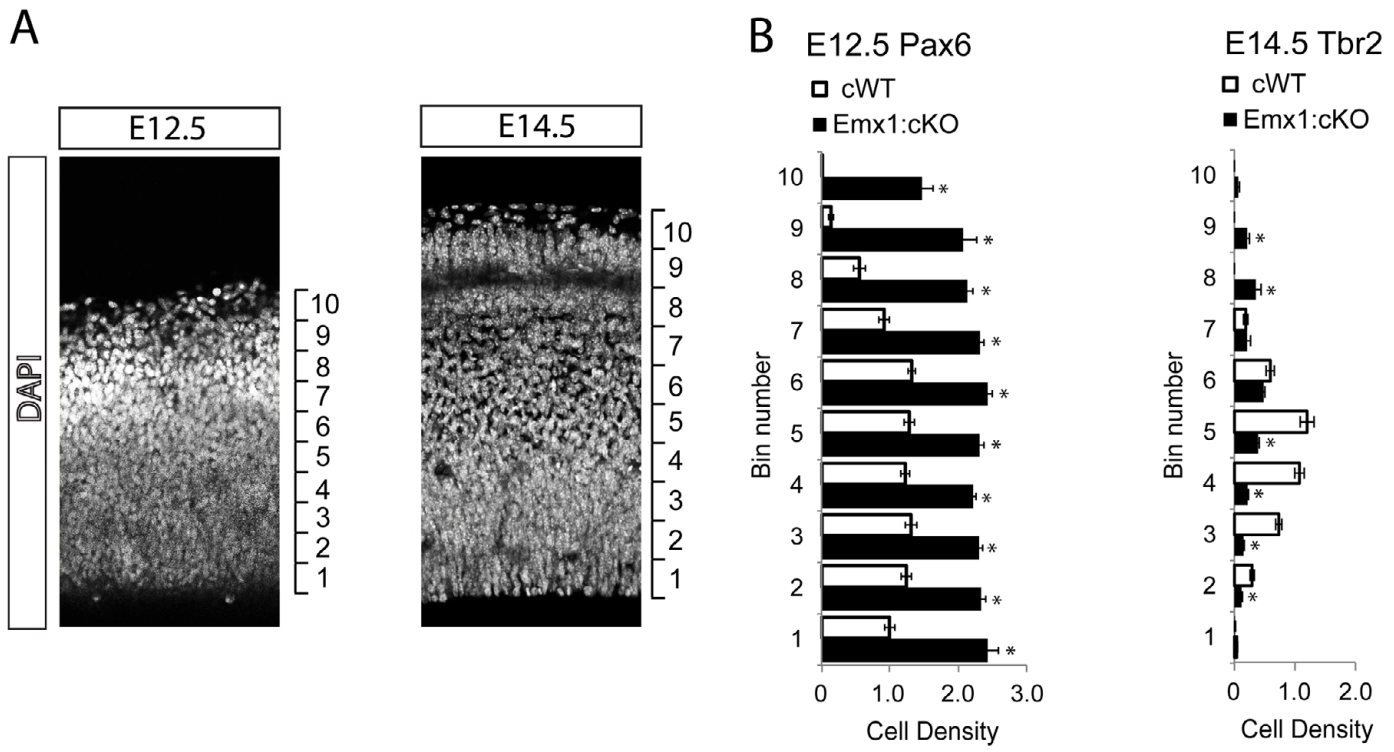

Fig. S6. Distribution of Pax6 and Tbr2 progenitors in the E12.5 and E14.5 cerebral cortex. (**A**) The thickness of E12.5 and E14.5 cerebral cortices were visualized by DAPI nuclear staining and divided into 10 equidistant bins to quantify distribution of distinct makers. (**B**) Quantified densities of Pax6+ or Tbr2+ cells in each bin of Emx1:cWT and Emx1:cKO cerebral cortices at each age. Data are mean±s.e.m.; **P*<0.01, Student's *t*-test, n=3/age group/genotype.

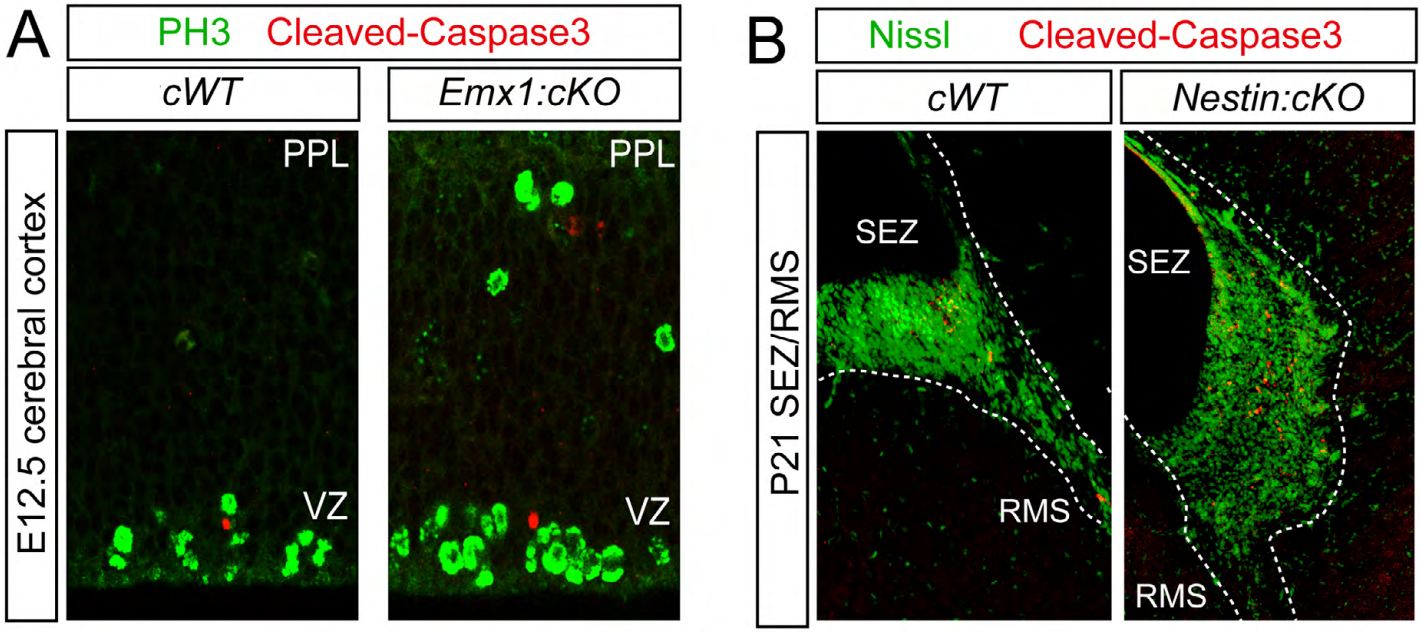

Fig. S7. Analysis of caspase-dependent apoptosis in conditionally Sp2-deleted embryonic cerebral cortex and postnatal SEZ/RMS. (**A**) Confocal images of tissue stained for cleaved caspase 3 (red) and PH3 (green) in the E12.5 cerebral cortex. The density and distribution of cleaved caspase 3-labeled apoptotic cells were indistinguishable in *Emx1:cWT* and *Emx1:cKO* cortices. (**B**) At P21, an increase in immunoreactivity for cleaved-caspase 3 (red) emerged within the cellular bulge revealed by Nissl stain (green) in Nestin:cKO compared with cWT SEZ and RMS.

Table S1. Mice purchased from the Jackson laboratory

Name	Jackson Laboratory ID	Catalogue #
Nestin-cre	B6.Cg-*Tg (Nes-cre)1Kln*/J	003771
tdTomato	B6.129S6-*Gt (ROSA) 26Sor*$^{tm14\ (CAG-tdTomato)\ Hze}$/J	007908
Emx1^{cre}	B6.129S2-*Emx1*$^{tm1(cre)Krj}$/J	005628

Antibody	Source	Dilution
rabbit anti-Ki67	Vision Biosystems	1:500
rabbit anti-PH3	Millipore	1:500
mouse anti- PH3	Abcam	1:500
mouse anti-BrdU	BD Bioscience	13:1000
guinea pig anti-Dcx	Millipore	1:1000
mouse anti-GFAP	Millipore	1:1000
mouse anti-NeuN	Millipore	1:1000
rabbit anti-S100_	Sigma	1:1000
rabbit anti-Dlx2	Gift of Dr. David Eisenstat	1:1000
rabbit anti-Gsx2	Gift of Dr. Kenny Campbell	1:4000
rabbit anti-Pax6	Millipore	1:500
rabbit anti-cleaved caspase3	Cell Signaling	1:1000
rabbit anti-BLBP	Millipore	1:500
rabbit anti-Tbr2	Abcam	1:500
Rabbit anti-NG2	Millipore	1:1000
Mouse anti-Tuj1	Covance	1:1000
Rabbit anti-Cux1	Santa Cruz	1:500
Rabbit anti-Ctip2	Abcam	1:500
Rat anti-BrdU	Abcam	1:200
chicken anti-GFP	Abcam	1:1000
rabbit anti-RFP	Abcam	1:1000
Goat anti-rabbit Alexa488	Invitrogen	1:1000
Goat anti-mouse Alexa488	Invitrogen	1:1000
Goat anti-chicken Alexa488	Invitrogen	1:1000
Goat anti-rabbit Cy3	Millipore	1:1000
Goat anti-mouse Cy3	Millipore	1:1000
Goat anti-rabbit Alexa647	Invitrogen	1:500
Goat anti-mouse Alexa647	Invitrogen	1:500
Goat anti-guinea pig Cy3	Millipore	1:1000

Table S2. Primary and secondary antibodies used in the study.

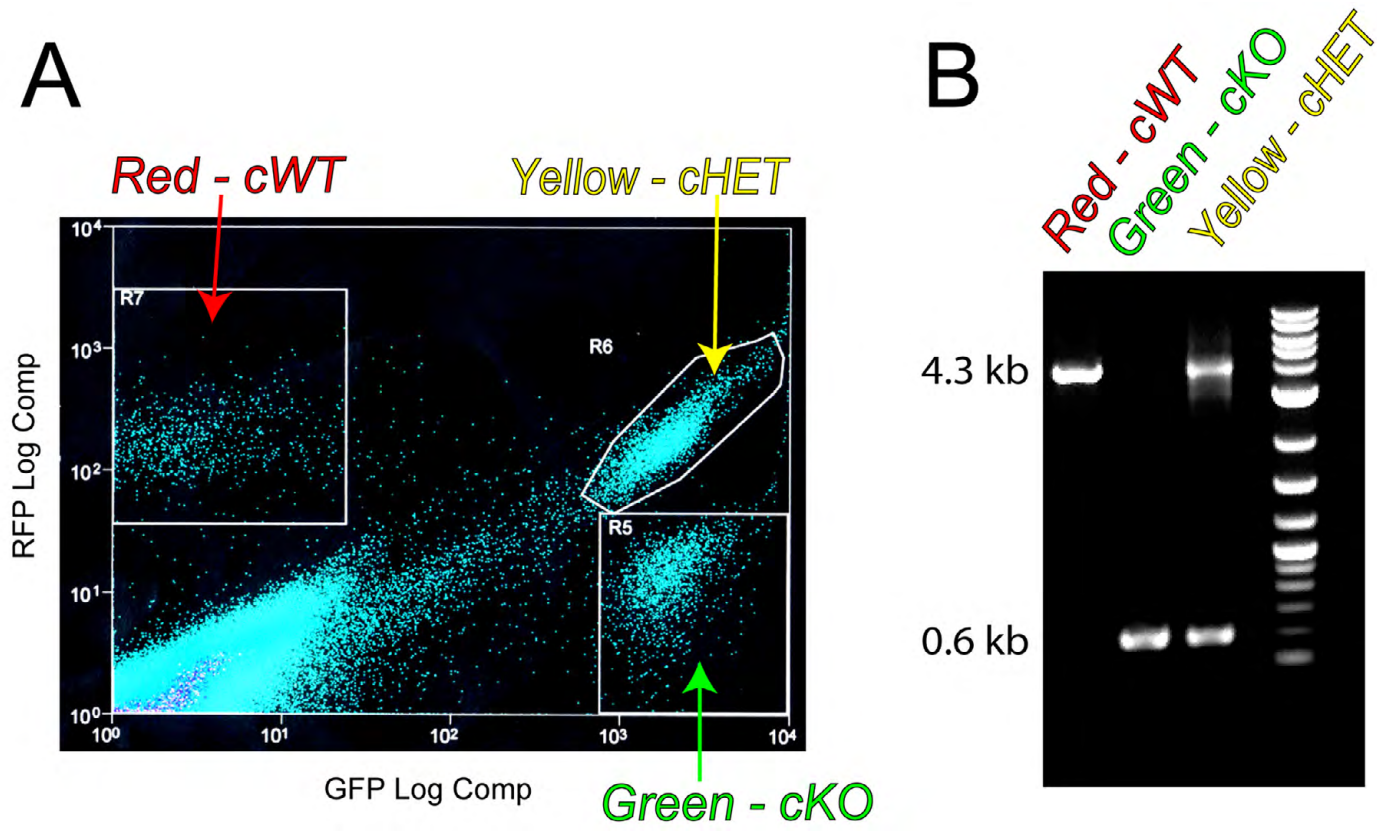

Fig. S3. Distinctly labeled MADM-11 cells faithfully carry allelic deletion of *Sp2* corresponding to expected combinatorial expression of fluorophores. (**A**) *Nestin-cre:Sp2* $^{F/+}$*:MADM-11* cells from P0 mice were harvested and isolated using fluorescence activated cell sorting. (**B**) PCR analysis of DNA confirmed genotypes of distinctly sorted populations corresponding to red=cWT, green=cKO and yellow=cHet genotypes.

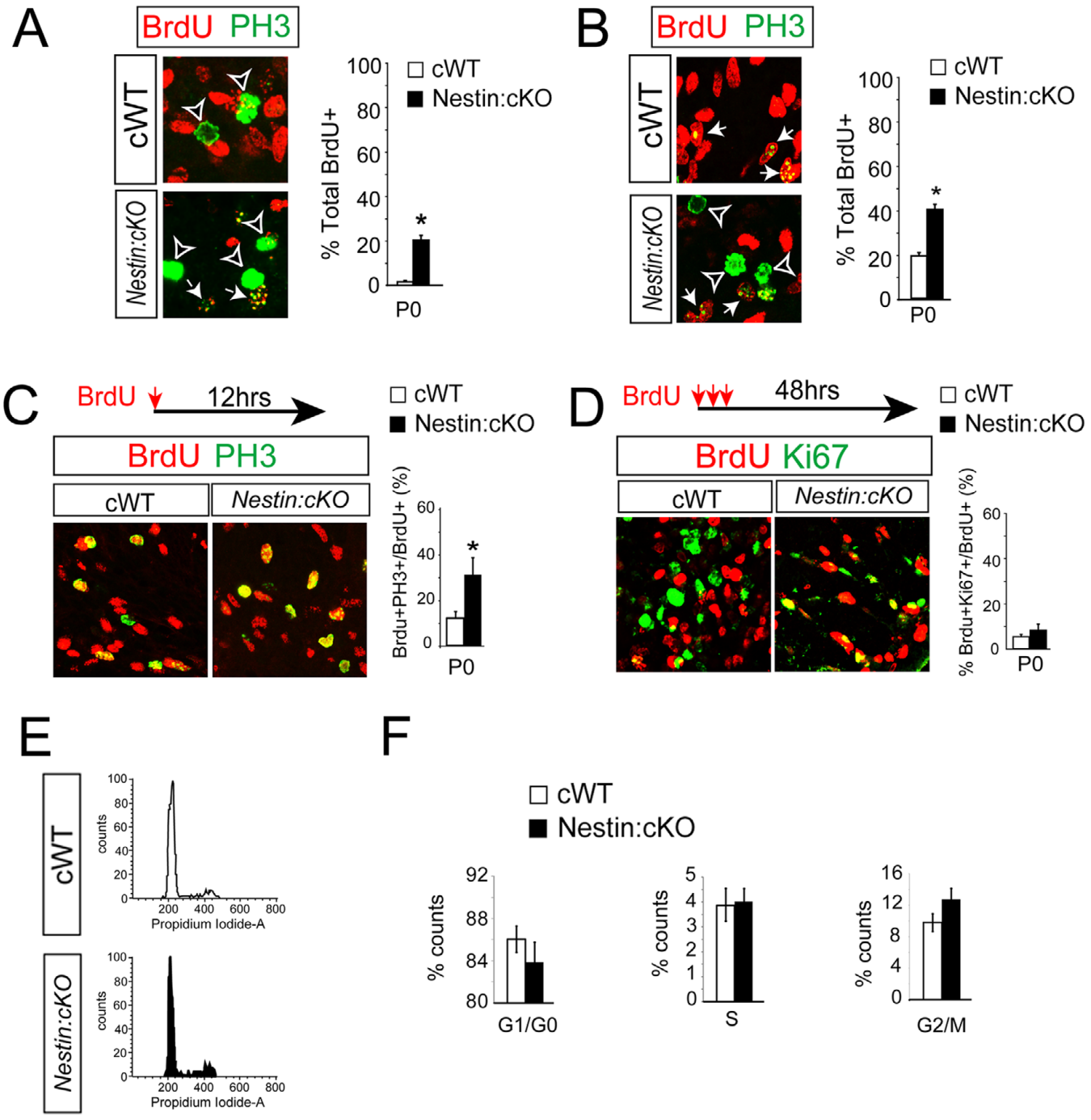

Fig. S4. Cell cycle progression from S-to-G2/M is disrupted in Nestin:cKO progenitors harvested at P0. (**A**) A 1-hour BrdU pulse-chase experiments allowed for identification of proliferating cells that progressed from S to G2/M phases of the cell cycle by co-labeling BrdU (red) with the M-phase marker PH3 (green; arrows). M-phase cells that did not incorporate BrdU during the 1-hour chase period were labeled as PH3+/BrdU negative (arrow heads). The proportion of BrdU+ cells in the SEZ and RMS of Nestin:cKO mice that progressed into G2/M (PH3+) was consistently and significantly higher compared with cWT progenitors at P0. (**B**) Four-hour BrdU pulse-chase experiments allowed for identification of proliferating Nestin:cKO progenitors that exhibit M phase perdurance. Arrows indicate BrdU+/PH3+ cells; arrowheads indicate BrdU-negative/PH3+ cells. Percentage of BrdU+/PH3+ cells among all BrdU incorporated cells is significantly increased in P0 mutant compared with the control. In addition, a significant fraction of PH3+ cells in the Nestin:cKO SEZ and RMS remained BrdU negative. (**C**) BrdU administration followed by 12 hours of chase allowed for indexing M-phase exiting. The percentage of BrdU+/PH3+ cells in the Nestin:cKO SEZ and RMS was significantly higher than in cWT brains. (**D**) To quantify cell cycle exiting, three pulses of BrdU were administered every 2 hours followed by a 48-hour survival period. In this regimen, BrdU immunoreactivity was combined with Ki67 staining in order to distinguish progenitors that had remained in, or re-entered, the cell cycle after 48 hours (BrdU+/Ki67+) from cells that had exited the cell cycle (BrdU+/Ki67 negative). Percentage of BrdU+/Ki67+ cells among all BrdU incorporated cells is higher in the Nestin:cKO SEZ/RMS compared with controls. For A-D, data are mean±s.e.m.; *P<0.05, Student's t-test, n=3/age group. (**E**,**F**) Flow cytometry for cell cycle analysis at P0. Data from cycling cells harvested from P0 SEZ and RMS illustrated higher proportion of cells in the G2/M phases in Nestin:cKOs. *P<0.01, Student's t-test, n=3/age group.

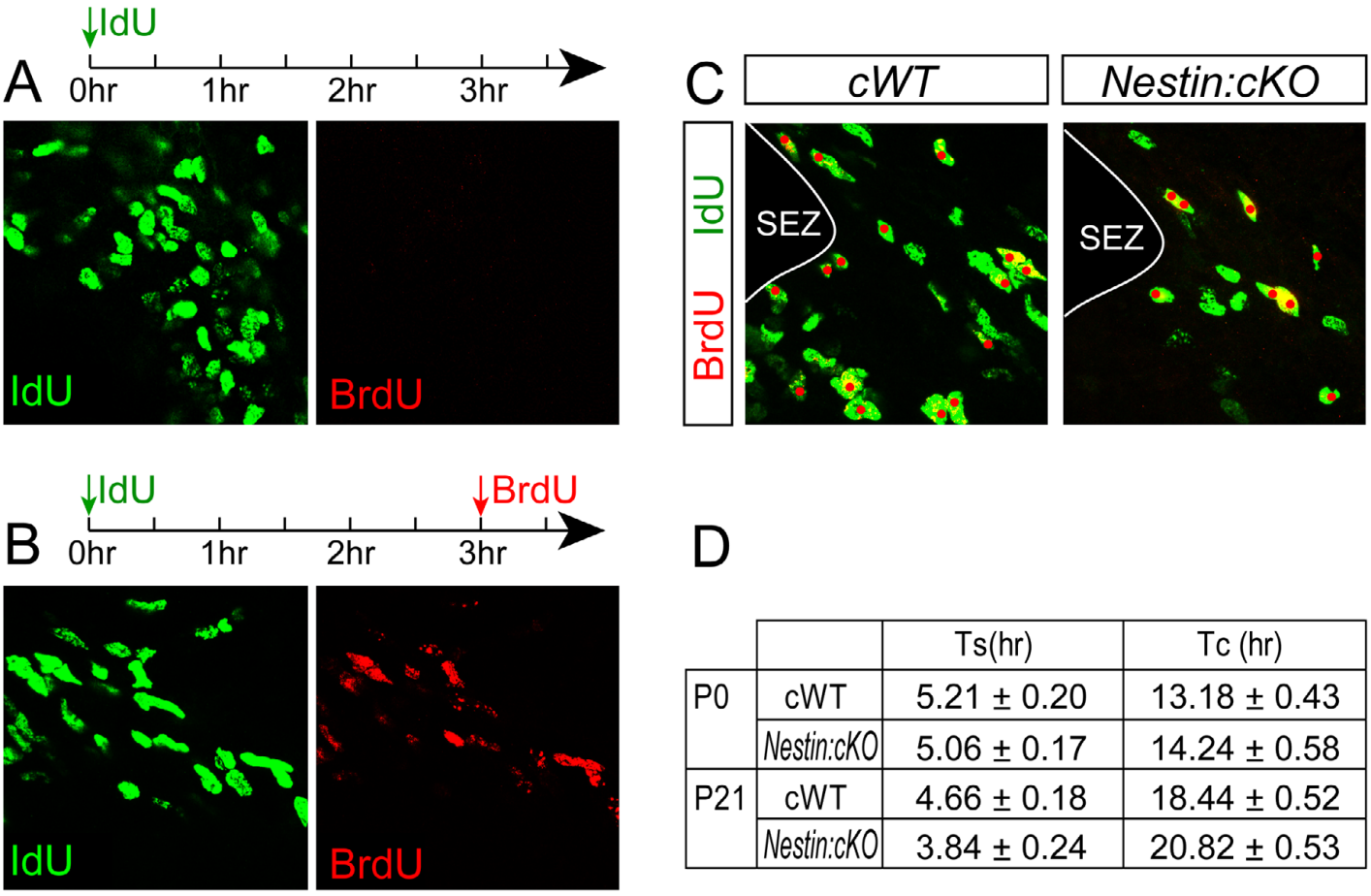

		Ts(hr)	Tc (hr)
P0	cWT	5.21 ± 0.20	13.18 ± 0.43
	Nestin:cKO	5.06 ± 0.17	14.24 ± 0.58
P21	cWT	4.66 ± 0.18	18.44 ± 0.52
	Nestin:cKO	3.84 ± 0.24	20.82 ± 0.53

Fig. S5. IdU/BrdU dual labeling for estimating the lengths of the S-phase and total cell cycle. (**A**) An antibody specific to BrdU failed to label IdU incorporated cells (green) in the absence of BrdU injection. (**B**) A pulse of IdU was followed by a pulse of BrdU 3 hours later that could be distinguished using an antibody that recognizes both BrdU and IdU (green), and one that is specific to BrdU (red). (**C**) Representative confocal micrographs of IdU (green) and BrdU (red) labeled nuclei in P21 cWT and Nestin:cKO SEZs. Red dots highlight IdU+/BrdU+ cells. (**D**) Estimated lengths of S (Ts) and total cell cycle (Tc) in the P0 and P21 wild-type and mutant SEZ progenitors. Data are mean±s.e.m., *n*=3/genotype/age.

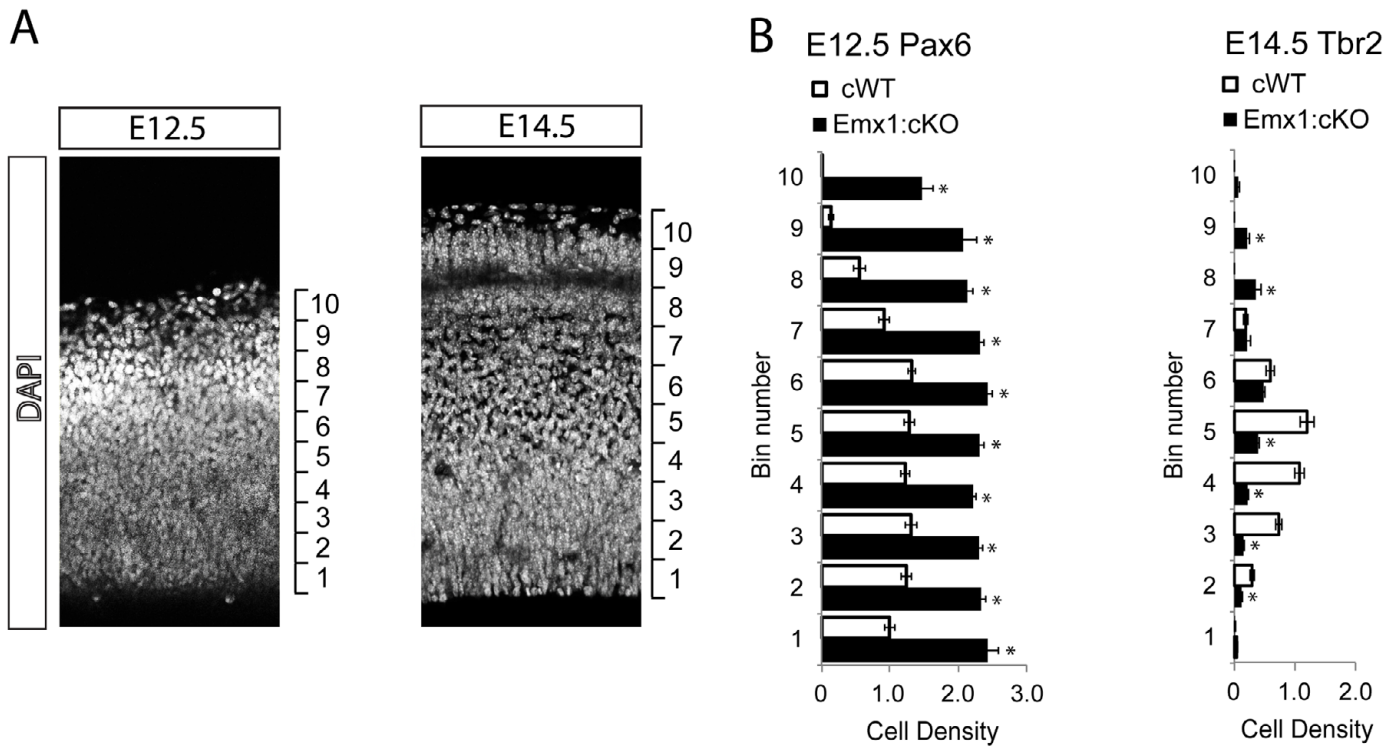

Fig. S6. Distribution of Pax6 and Tbr2 progenitors in the E12.5 and E14.5 cerebral cortex. (**A**) The thickness of E12.5 and E14.5 cerebral cortices were visualized by DAPI nuclear staining and divided into 10 equidistant bins to quantify distribution of distinct makers. (**B**) Quantified densities of Pax6+ or Tbr2+ cells in each bin of Emx1:cWT and Emx1:cKO cerebral cortices at each age. Data are mean±s.e.m.; **P*<0.01, Student's *t*-test, n=3/age group/genotype.

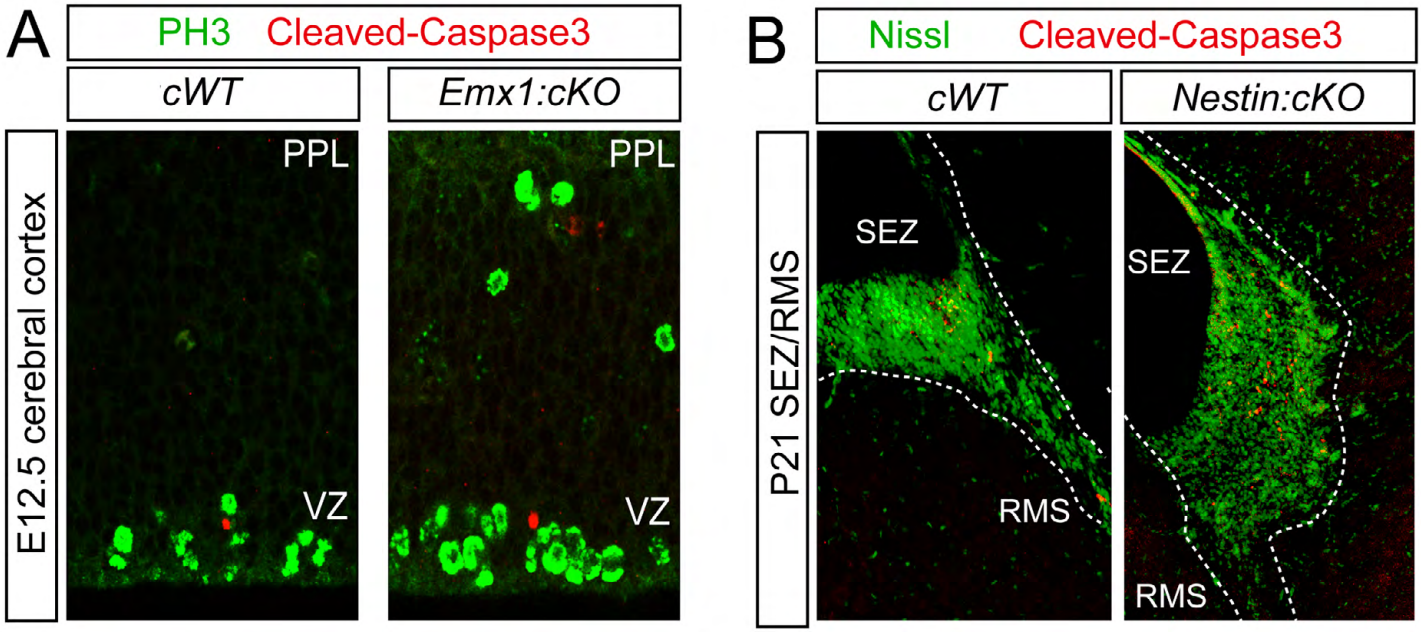

Fig. S7. Analysis of caspase-dependent apoptosis in conditionally Sp2-deleted embryonic cerebral cortex and postnatal SEZ/RMS. (**A**) Confocal images of tissue stained for cleaved caspase 3 (red) and PH3 (green) in the E12.5 cerebral cortex. The density and distribution of cleaved caspase 3-labeled apoptotic cells were indistinguishable in *Emx1:cWT* and *Emx1:cKO* cortices. (**B**) At P21, an increase in immunoreactivity for cleaved-caspase 3 (red) emerged within the cellular bulge revealed by Nissl stain (green) in Nestin:cKO compared with cWT SEZ and RMS.